

Toward Reliable Human Pose Forecasting with Uncertainty

Saeed Saadatnejad Mehrshad Mirmohammadi* Matin Daghyani* Parham Saremi*
 Yashar Zoroofchi Benisi* Amirhossein Alimohammadi* Zahra Tehraninasab*
 Taylor Mordan Alexandre Alahi

Abstract

Recently, there has been an arms race of pose forecasting methods aimed at solving the spatio-temporal task of predicting a sequence of future 3D poses of a person given a sequence of past observed ones. However, the lack of unified benchmarks and limited uncertainty analysis have hindered progress in the field. To address this, we first develop an open-source library for human pose forecasting, featuring multiple models, datasets, and standardized evaluation metrics, with the aim of promoting research and moving toward a unified and fair evaluation. Second, we devise two types of uncertainty in the problem to increase performance and convey better trust: 1) we propose a method for modeling aleatoric uncertainty by using uncertainty priors to inject knowledge about the behavior of uncertainty. This focuses the capacity of the model in the direction of more meaningful supervision while reducing the number of learned parameters and improving stability; 2) we introduce a novel approach for quantifying the epistemic uncertainty of any model through clustering and measuring the entropy of its assignments. Our experiments demonstrate up to 25% improvements in accuracy and better performance in uncertainty estimation.

1. Introduction

The task of human pose forecasting consists in predicting a sequence of future 3D poses of a person, given a sequence of past observed ones. It has attracted significant attention in recent years due to its critical applications in autonomous vehicles [43], human-machine interaction [11], and healthcare [66]. The field is now witnessing an arms race of forecasting models using different architectures that have shown increasing performances [37, 46, 44, 59, 41].

Forecasting human poses is a difficult problem with multiple challenges to solve: it mixes both spatial and temporal reasoning, with a huge variability in scenarios; and human

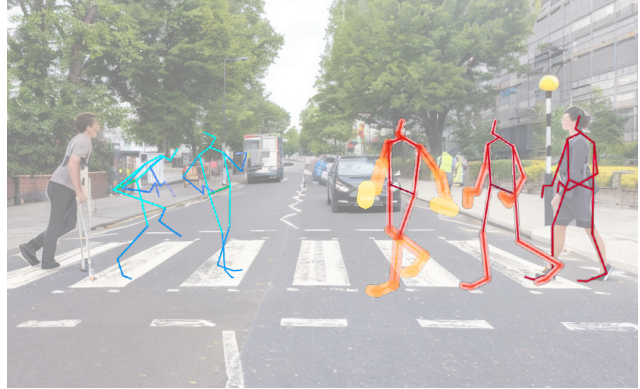


Figure 1: We propose to model two kinds of uncertainty: 1) aleatoric uncertainty, learned by our model to capture the temporal evolution of uncertainty, which becomes more prominent over time, as depicted by the lighter colors and thicker bones for the right person; 2) epistemic uncertainty to detect out-of-distribution forecast poses coming from unseen scenarios in training, such as for the left person.

behavior is difficult to predict, as it changes in dynamic and multi-modal ways to react to its environment. To guarantee safe interactions with humans, robots should not only predict human motions, but also identify scenarios in which they are uncertain [33, 5, 38, 63], and act accordingly. Fig. 1 illustrates a pose forecasting scenario. Without an uncertainty measure, all the forecast poses are considered valid. However, uncertainty measures can detect unconfident outputs and treat them with more caution. Recently, several works have shown the benefits of estimating uncertainty for classification [38, 63] and regression tasks [33, 5], but how to apply this principle to pose forecasting is not yet studied.

In this paper, we present two solutions to capture the uncertainty of pose forecasting models from two important perspectives. The first one deals with the aleatoric uncertainty, *i.e.*, the irreducible intrinsic uncertainty in the data. We reformulate the pose forecasting objective function to capture the aleatoric uncertainty. To reduce the number of learned parameters and improve stability, we introduce uncertainty priors based on our knowledge about the uncer-

The research was conducted in VITA laboratory at EPFL.
 e-mail: saeed.saadatnejad at epfl.ch

* Equal contribution as the second authors.

tainty, *e.g.*, that the uncertainty increases with time. We then train the forecasting model with the new objective function. This allows the model to focus its capacity to learn forecasting at shorter time horizons, where uncertainty is lower and learning is more meaningful, compared to longer ones that are intrinsically much harder and uncertain to forecast.

The second one is about epistemic uncertainty which shows the model’s lack of knowledge. To this end, we define a model-agnostic uncertainty metric as an indicator of the certainties and trustability of pose forecasting models in the real world. Unlike previous methods which require accessing model [19] (*i.e.*, white-box methods) or are specific to certain models [63], our approach does not require access to the model (*i.e.*, black-box approach) and is model-agnostic. Since there is no label for motions, we train a deep clustering network to learn the distribution of common poses and measure the dissimilarity between the predictions’ embeddings and cluster centers. We apply our proposed uncertainty methods to several models from the literature and evaluate them on three well-known datasets (Human3.6M [28], AMASS [42], 3DPW [65]) and achieve up to 25% improvement leveraging the aleatoric uncertainty and better performance in detecting out-of-distribution forecast poses using epistemic uncertainty.

Thanks to the large interest in pose forecasting, the field is advancing at a quick pace. However, this happens at the cost of unfair and non-unified evaluations. Concurrent papers all use disparate metrics and dataset setups to report their results, leading to ambiguities and errors in interpretation. In an effort to mitigate these discrepancies, we finally release an open-source library for human pose forecasting named *unposed*¹ with more than 10 models, 3 datasets and 5 metrics from the literature, all implemented and tested in a standardized way, in order to ease the implementation and evaluation of new ideas and promote research in this field. To summarize, our contributions are three-fold:

- We propose a method for incorporating priors to estimate the aleatoric uncertainty in human pose forecasting and demonstrate its efficacy in improving several state-of-the-art models on multiple datasets;
- We propose a model-agnostic metric of quantifying epistemic uncertainty to evaluate models in unseen situations, outperforming previous methods;
- We develop and publicly release an open-source library for human pose forecasting.

2. Related works

Human pose forecasting: While the literature has extensively examined the forecasting of a sequence of future

center positions at a coarse-grained level [34, 55, 4] or a sequence of bounding boxes [7, 56], our focus in this work is on a more fine-grained forecasting *i.e.*, pose. Additionally, we limit our focus to the observation sequence alone, rather than incorporating context information [9, 25, 13], social interactions [1], or action class [8]. Many approaches have been proposed for human pose forecasting, with some using feed-forward networks [37] and many others using Recurrent Neural Networks (RNNs) to capture temporal dependencies [18, 31, 47, 10, 20, 12]. To better capture spatial dependencies of body poses, Graph Convolutional Networks (GCNs) have been utilized [46, 14, 44, 39], along with separating temporal and spatial convolution blocks and using trainable adjacency matrices [59, 75]. Attention-based approaches have also gained interest for modeling human motion, showing improvement with a spatio-temporal self-attention module [44]. More recently, forecasting in multiple stages [41] and a diffusion stochastic model with a transformer-based architecture [57] have been proposed. We can categorize all previous works into stochastic and deterministic models. Stochastic models [73, 3, 2, 58, 40, 45, 57] can give diverse predictions but we mainly focus on deterministic models [44, 41, 59, 15] as they provide more accurate predictions. Given the growing interest in this field, we believe that greater attention should be paid to uncertainty estimation in this task.

Uncertainty in pose forecasting: Knowing when a model does not know, *i.e.* uncertain, is important to improve trustworthiness and safety [48]. Traditionally, uncertainty in deep learning is divided into data (aleatoric) and model (epistemic) uncertainty [33]. The aleatoric originates from the intrinsic noise and inherent uncertainty of data and cannot be reduced by improving the model, while the epistemic uncertainty shows the model’s weakness in recognizing the underlying pattern of the data and can be reduced by enhancing the network architecture or increasing data. Many methods have been proposed to estimate and utilize these types of uncertainty in various tasks, including image classification [19], semantic segmentation [32], and natural language processing [70]. It has also been widely explored in pose estimation from images and videos [22, 35, 30, 74, 50, 24], visual navigation and trajectory forecasting tasks [67, 61, 29, 27, 52, 54, 16] but not yet studied in human pose forecasting which includes spatio-temporal relationships modeling. We will show how modeling the uncertainty can improve accuracy.

Moreover, it is important to measure the epistemic uncertainty of models when going to be used in the real world. Bayesian Neural Networks (BNNs) have conventionally been used to formulate uncertainty by defining probability distributions over the model parameters [49]. However, the intractability of these distributions has led to the development of alternative approaches to perform approximate

¹<https://github.com/vita-epfl/unposed>

Bayesian inference for uncertainty estimation. One popular approach is Variational Inference [21, 6] because of their scalability. One important example is the technique of Monte Carlo (MC) dropout [19], which involves applying dropout [60] at inference time to model the parameters of the network as a mixture of multivariate Gaussian distributions with small variances. However, all those methods need to access the model and are not model-agnostic. Calibration [23] is another approach, but it requires the model to provide probabilities and deep neural networks have been shown to be poorly calibrated. One way to evaluate model reliability is by measuring the distance between a new sample and the training samples using a deep deterministic network, a technique that has been effective in image classification [38, 63]. However, this approach measures the uncertainty for their own model and is not applicable to measuring the uncertainty of different models. In contrast, Deep Ensembles [36] can measure the uncertainty of different models by training multiple neural networks independently and averaging their outputs at inference time. However, this method can be computationally expensive and slow. In this study, we concentrate on the model’s output and define epistemic uncertainty as the extent to which the model’s forecast resemble the training distribution. This way, we can measure the uncertainty in a black-box manner.

3. Aleatoric uncertainty in pose forecasting

Pose forecasting models usually take as input a sequence x of 3D human poses with J joints in O observation time frames, and predict another sequence \hat{y} of 3D poses to forecast its future y in the next T time frames. In addition to this, we also want a model to estimate its aleatoric uncertainty u along with the predicted poses \hat{y} , to indicate how reliable these can be.

For this, we model the probability distribution of the error, *i.e.*, the euclidean distance between ground truths y and forecasts \hat{y} , with an exponential distribution following [5]:

$$\|y - \hat{y}\|_2 \sim \text{Exp}(\alpha), \quad (1)$$

where α is the distribution parameter to be selected. Its log-likelihood therefore writes

$$\ln p(\|y - \hat{y}\|_2) = \ln \alpha - \alpha \|y - \hat{y}\|_2. \quad (2)$$

We then define the aleatoric uncertainty as $u := -\ln \alpha$, and set it as a learnable parameter for the model. When training the model with maximum likelihood estimation, the loss function \mathcal{L} to minimize is then given by

$$\begin{aligned} \mathcal{L}(y, \hat{y}, u) &= -\ln p(\|y - \hat{y}\|_2) \\ &= e^{-u} \|y - \hat{y}\|_2 + u. \end{aligned} \quad (3)$$

We consider pose forecasting as a multi-task learning problem with task-dependant uncertainty, *i.e.*, independent

of the input sequences x . There are several ways to define tasks in this manner, *e.g.*, by separating them based on time frames, joints, actions (if the datasets provide them), or any other combination of them. In the following, we consider dividing tasks based on time and joints². In this case, for each future time frame t and joint j , the model predicts an uncertainty estimate u_t^j associated with its 3D joint forecasts \hat{y}_t^j . This formulation yields the corresponding loss function:

$$\mathcal{L}_{total}(y, \hat{y}, u) = \sum_{\substack{t=1 \dots T \\ j=1 \dots J}} e^{-u_t^j} \left\| y_t^j - \hat{y}_t^j \right\|_2 + u_t^j, \quad (5)$$

where T refers to the number of prediction frames and J is the number of joints.

Since the loss function (Eq. (5)) weighs the error $\left\| y_t^j - \hat{y}_t^j \right\|_2$ based on the aleatoric uncertainty $e^{-u_t^j}$, it forces the model to focus its capacity to points with lower aleatoric uncertainty. In particular, we expect short time horizons to have lower uncertainty, and therefore to present better improvements than longer ones.

Unfortunately, learning all aleatoric uncertainty values u_t^j independently leads to an unstable training. To address this issue, we introduce uncertainty priors F , in order to inject knowledge about the aleatoric uncertainty behavior and stabilize the training. For this, we choose a family F of functions parameterized by a given number of parameters θ . Instead of learning all uncertainty values u_t^j independently, the model now only learns θ , which can be chosen to be of a smaller size so as to ease the training. With a learned θ^* , the uncertainty values u_t^j are obtained with the function $F(\theta^*)$:

$$u_t^j = F(\theta^*)(j, t). \quad (6)$$

It is noticeable that this framework generalizes the previous case (without prior) by setting F to yield a separate parameter for each uncertainty value:

$$u_t^j = \text{Id}(\theta^*)(j, t) = \theta_t^j. \quad (7)$$

Intuitively, the more parameters F has, the more scenarios it can represent, but at the cost of stability. We, therefore, compare several choices for F , with variable numbers of learnable parameters as different trade-offs between ease of learning and representation power. We select three functions that constrain the temporal evolution of aleatoric uncertainty, independently for each joint. We select functions with a logarithmic shape due to the observed exponential behavior in error evolution over time. The first one, Sig_3 , is a sigmoid function used to ensure that uncertainty only increases with time, and has three parameters per joint to

²Extending the formulation to other task definitions should be straightforward.

control this behavior:

$$u_t^j = \text{Sig}_3(\theta)(j, t) = \frac{\theta_2^j}{1 + e^{-\theta_0^j(t-\theta_1^j)}}. \quad (8)$$

Then we leverage Sig_5 , which is a generalized version of the sigmoid function [53] with 5 parameters per joint:

$$u_t^j = \text{Sig}_5(\theta)(j, t) = \theta_0^j + \frac{\theta_1^j}{1 + ab + (1-a)c}, \quad (9)$$

where the terms a , b and c are defined by

$$a = \frac{1}{1 + e^{-\frac{2\theta_2^j\theta_4^j}{|\theta_2^j+\theta_4^j|}(\theta_3^j-t)}}, \quad (10)$$

$$b = e^{\theta_2^j(\theta_3^j-t)}, \quad (11)$$

$$c = e^{\theta_4^j(\theta_3^j-t)}. \quad (12)$$

We also compare with a more generic polynomial function Poly_d of degree d , which has $d+1$ learnable parameters per joint and constrain the uncertainty less:

$$u_t^j = \text{Poly}_d(\theta)(j, t) = \theta_0^j + \theta_1^j t + \theta_2^j t^2 + \dots + \theta_d^j t^d. \quad (13)$$

4. Epistemic uncertainty in pose forecasting

We introduced aleatoric uncertainty to address the uncertainty in the data in the previous section. We now address the epistemic uncertainty to capture the model’s uncertainty due to the lack of knowledge. We want to quantify the intuition that the models with predicted motions dissimilar to the training distribution in the latent representation are less reliable and, therefore, should be treated with caution. We improve upon existing literature by introducing temporal modeling and clustering in epistemic uncertainty. Specifically, we use an LSTM-based autoencoder (Fig. 2) to encode the spatio-temporal relation between various frames in the latent representation and we rely on clustering on that space as there are no predefined motion classes.

In the following sections, we first explain how to estimate the number of motion clusters K and train the deep embedded clustering. We then illustrate how to measure the epistemic uncertainty.

4.1. Determining the number of motion clusters

Determining K , the number of clusters, is essential since it corresponds to the diversity of motions in the training dataset. An optimal K , therefore, captures the diversity in the training dataset while also reducing the time complexity of our subsequent algorithms.

We first train an LSTM auto-encoder (Fig. 2) to learn low dimensional embeddings Z by minimizing the reconstruction loss L_{recons} over the training dataset. We then

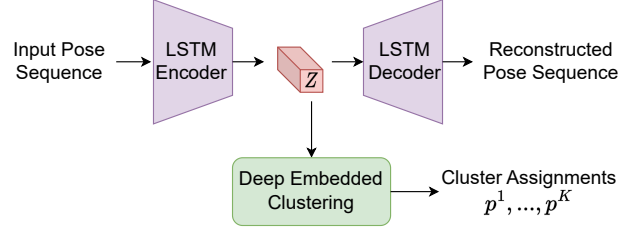


Figure 2: The motion is encoded into a well-clustered representation space Z by our LSTM encoder-decoder. The probabilities of the cluster assignments are provided by our deep embedded clustering on that space to estimate the epistemic uncertainty.

follow DED [69] which uses t-SNE [64] to reduce Z to a 2-dimensional feature vector z' . Subsequently, local density ρ_i and delta δ_i for each data point are calculated:

$$\rho_i = \sum_j \chi(d_{ij} - d_c),$$

$$\delta_i = \min_{j:\rho_j > \rho_i} d_{ij}, \quad (14)$$

where $\chi(\cdot) = 1$ if $\cdot < 0$ else $\chi(\cdot) = 0$, d_{ij} is the distance between z'_i and z'_j , and d_c is the cut-off distance. We then define $\gamma_i = \rho_i \delta_i$ similar to [26, 68]. A larger γ_i corresponds to a greater likelihood of being chosen as a cluster center; however, the number of clusters still remains a hyperparameter. We fully automate it by defining r_i as the gap between two γ_i and γ_{i+1} values (where $\gamma_{i+1} < \gamma_i$):

$$r_i = \frac{\gamma_i}{\gamma_{i+1}}, i \in [1, N-1]. \quad (15)$$

We set $K = \text{argmax}(r_i)$ since γ_K represents the largest shift in likelihood of a sample being a cluster itself.

4.2. Deep embedded clustering

Having identified the number of clusters, we now learn the optimal deep clustering of our embedding. We initialize the cluster centers $\{\mu^k\}_{k=1}^K$ using the K-means algorithm on the feature space. We then minimize the clustering loss $L_{cluster}$ as defined in DEC [71] jointly with the reconstruction loss in order to learn the latent representation as well as clustering. We incorporated the reconstruction loss into the loss function to act as a regularizer and prevent the collapse of the network parameters. The loss function is defined as:

$$L = L_{cluster} + \lambda L_{recons}, \quad (16)$$

where λ is the regularization coefficient. Finally, when the loss is converged, we fine-tune the trained network using the cross-entropy loss on the derived class labels in order to make clusters more compact.

4.3. Estimating Epistemic Uncertainty

Now, we estimate the epistemic uncertainty of a given forecasting model. Specifically, for each example, denote the probability of assignment to the k th cluster by p^k . The epistemic uncertainty is then calculated as follows:

$$EpU = \frac{1}{N} \sum_{i=1}^N \text{entropy}(p_i^1, \dots, p_i^K), \quad (17)$$

where N is the size of the dataset. In other words, a model that does not generate outputs close to the motion clusters is considered uncertain.

5. Experiments

5.1. Datasets

Human3.6M [28] contains 3.6 million body poses. It comprises 15 complex action categories, each one performed by seven actors individually. The validation set is subject-11, the test set is subject-5, and all the remaining five subjects are training samples. The original 3D pose skeletons in the dataset consist of 32 joints. Similar to previous works, we have 10/50 observation frames, 25 forecast frames down-sampled to 25 fps, with the subset of 22 joints to represent the human pose. We train our models on all action classes at the same time.

AMASS (The Archive of Motion Capture as Surface Shapes) [42] unifies 18 motion capture datasets totaling 13,944 motion sequences from 460 subjects performing a variety of actions. We use 50 observation frames down-sampled to 25fps with 18 joints, similar to previous works.

3DPW (3D Poses in the Wild) [65] is the first dataset with accurate 3D poses in the wild. It contains 60 video sequences taken from a moving phone camera. Each pose is described as an 18-joint skeleton with 3D coordinates similar to AMASS dataset. We use the official instructions to obtain training, validation, and test sets.

5.2. Evaluation Metrics

We measure the accuracy in terms of MPJPE (Mean Per Joint Position Error) in millimeters (mm) per frame:

$$MPJPE = \frac{1}{J} \sum_{j=1}^J \left\| \hat{y}_t^j - y_t^j \right\|_2, \quad (18)$$

and report A-MPJPE as the average for all frames when needed. We also report EpU as defined in Eq. (17).

5.3. Baselines

We apply our approach to several recent methods that are open-source [44, 41, 59] and compare with the performance on. Note that we follow their own training setup in which

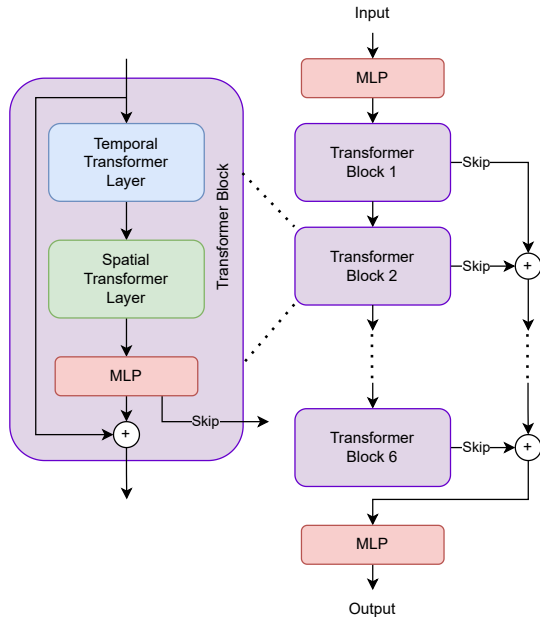


Figure 3: ST-Trans consists of 2 MLP layers and 6 Transformer Blocks with skip connections. Each Transformer Block contains two cascaded temporal and spatial transformers to capture the spatio-temporal features of data.

some use 10 frames of observation [59, 41, 15] and the rest 50 frames of observation [44, 47, 37, 46]. We report the results obtained from the trained model of STARS* [72] as documented on their GitHub page. We also consider *Zero-Vel*, which outputs the last observed pose as the forecast for all future poses as a simple and competitive baseline.

Inspired by the common trend to treat sequences with Transformers, we have designed our own simple transformer-based architecture referred to as *ST-Trans*. We followed the best practices proposed in [62] and adapted it to the task of pose forecasting. As depicted in Fig. 3, it is composed of several identical residual layers, each layer consists of a spatial and a temporal transformer encoder to learn the spatio-temporal dynamics of data utilizing the attention mechanism.

5.4. Aleatoric uncertainty

We first show the impact of aleatoric Uncertainty-Aware Loss (pUAL) with the prior Sig_5 to several models from the literature and our ST-Trans. Tab. 1 shows the overall results on Human3.6M [28]. To have a fair evaluation between all models, we adapt HRI [44] to predict 25 frames in one step (denoted as HRI*). We observe that all methods get better results when taking aleatoric uncertainty into account during learning, therefore confirming the need for aleatoric uncertainty estimation. It is noticeable that pUAL gives bet-

Model	Venue	80 ms	160 ms	320 ms	400 ms	560 ms	720 ms	880 ms	1000 ms
Zero-Vel	-	23.8	44.4	76.1	88.2	107.4	121.6	131.6	136.6
Res. Sup. [47]	CVPR'17	25.0	46.2	77.0	88.3	106.3	119.4	130.0	136.6
ConvSeq2Seq [37]	CVPR'18	16.6	33.3	61.4	72.7	90.7	104.7	116.7	124.2
LTD-50-25 [46]	ICCV'19	12.2	25.4	50.7	61.5	79.6	93.6	105.2	112.4
MSR-GCN [15]	ICCV'21	12.0	25.2	50.4	61.4	80.0	93.9	105.5	112.9
STARS* [72]	ECCV'22	12.0	24.6	49.5	60.5	78.6	92.6	104.3	111.9
ST-S-GCN [59]	ICCV'21	17.7	33.9	56.3	67.5	85.1	99.4	109.9	117.0
ST-S-GCN + pUAL (ours)		13.2	27.1	54.7	66.2	84.5	97.9	109.3	115.7
gain		25.4 %	20.1 %	2.8 %	1.9 %	0.7 %	1.5 %	0.5 %	1.1 %
HRI* [44]	ECCV'20	12.7	26.1	51.5	62.6	80.8	95.1	106.8	113.8
HRI* + pUAL (ours)		11.6	25.3	51.2	62.2	80.1	93.7	105.0	112.1
gain		8.7 %	3.1 %	0.6 %	0.6 %	0.9 %	1.5 %	1.7 %	1.5 %
PGBIG [41]	CVPR'22	10.3	22.6	46.6	57.5	76.3	90.9	102.7	110.0
PGBIG + pUAL (ours)		9.6	21.7	46.0	57.1	75.9	90.3	102.1	109.5
gain		6.8 %	4.0 %	1.3 %	0.7 %	0.5 %	0.7 %	0.6 %	0.5 %
ST-Trans		13.0	27.0	52.6	63.2	80.3	93.6	104.7	111.6
ST-Trans + pUAL (ours)		10.4	23.4	48.4	59.2	77.0	90.7	101.9	109.3
gain		20.0 %	13.3 %	8.0 %	6.3 %	4.1 %	3.1 %	2.7 %	2.1 %

Table 1: Comparison of our method on Human3.6M [28] in MPJPE (mm) at different prediction horizons. +pUAL refers to models where aleatoric uncertainty is modeled.

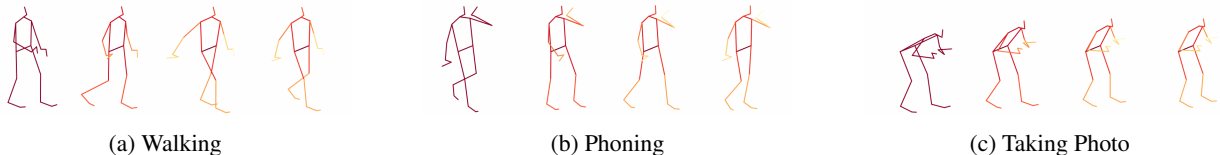


Figure 4: Qualitative results on Human3.6M [28] different actions. Higher aleatoric uncertainty is shown with a lighter color. Uncertainty of any bone is considered as its outer joint’s uncertainty assuming the hip is the body center. We observe that the estimated uncertainty increases over time, with joints farther away from the body center associated with higher uncertainties.

ter improvements for shorter prediction horizons, *e.g.*, up to 25.4 % and 20.1 % for ST-S-GCN [59] at horizons of 80 ms and 160 ms, which correspond to the less uncertain time frames, where pUAL focuses training more (smaller discount in the loss function, as seen in Eq. (5)). At the same time, adding pUAL does not degrade the performances at longer horizons. Examples of predicted 3D pose sequences using pUAL are depicted in Fig. 4, and show that the estimated uncertainty increases over time, with joints farther away from the body center associated with higher uncertainties. Moreover, we report the performances of the models on AMASS and 3DPW datasets in Tab. 2. Again, we observe that modeling aleatoric uncertainty leads to more accurate predictions, especially at shorter horizons, with improvements up to 14.1 % on AMASS and up to 9.0 % on 3DPW for ST-Trans at a horizon of 160 ms.

We argue that modeling the aleatoric uncertainty leads

to more stable training. In order to demonstrate this, we conduct five separate trainings of ST-Trans and present in Fig. 5 the A-MPJPE values along with their respective standard deviations for each epoch, which we refer to as stability. The plot highlights that the model with pUAL is more stable across runs, as indicated by a lower variance. Moreover, we compute AP-MPJPE, which is the average pairwise distance of predicted motions in terms of MPJPE, and observe that it decreases from 24.2 mm to 20.3 mm when pUAL loss is added, showing again lower variance in the output of the model.

So far, results have been reported using the Sig_5 uncertainty prior (Eq. (9)) to model the time and joint (T, J) aleatoric uncertainty. In Tab. 3, we report the performances of other choices on Human3.6M, and compare against using a single prior Sig_5 for all joints (only time dependency T) and other priors $\text{Sig}_3, \text{Poly}_9$. The results show again

Model	AMASS				3DPW			
	160 ms	400 ms	720 ms	1000 ms	160 ms	400 ms	720 ms	1000 ms
Zero-Vel	56.4	111.7	135.1	119.4	41.8	79.9	100.5	101.3
ConvSeq2Seq [37]	36.9	67.6	87.0	93.5	32.9	58.8	77.0	87.8
LTD-10-25 [46]	20.7	45.3	65.7	75.2	23.2	46.6	65.8	75.5
STS-GCN [59]	20.7	43.1	59.2	68.7	20.8	40.3	55.0	62.4
STS-GCN + pUAL (ours)	20.4	42.4	59.1	68.1	20.5	40.0	54.8	62.2
HRI [44]	20.7	42.0	58.6	67.2	22.8	45.0	62.9	72.5
HRI + pUAL (ours)	19.9	41.4	58.1	66.5	22.2	44.6	62.4	72.2
ST-Trans	21.3	42.5	58.3	66.6	24.5	47.4	64.6	73.8
ST-Trans + pUAL (ours)	18.3	39.7	56.5	66.7	22.3	45.7	63.6	73.2

Table 2: Comparison of our proposed method on AMASS [42] and 3DPW [65] in MPJPE (mm) at different prediction horizons. +pUAL refers to models where aleatoric uncertainty is modeled. The models were only trained on AMASS.

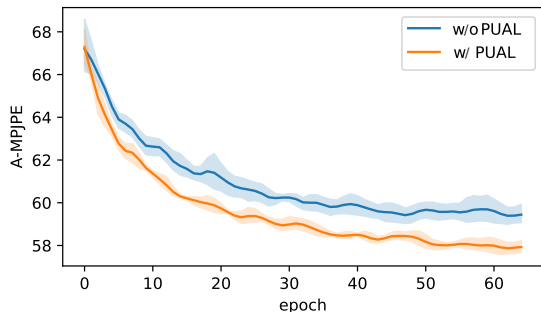


Figure 5: A-MPJPE and its standard deviation (stability) in training epochs for 5 trained models. The model with pUAL has a lower variance, meaning a more stable training.

Uncertainty prior (tasks)	Number of parameters	stability	ST-Trans	HRI*	STS-GCN
None	-	0.643	111.6	113.8	117.0
Id (T, J)	25 · 22	0.557	109.3	114.6	115.8
Poly ₉ (T, J)	10 · 22	0.505	110.3	114.7	118.1
Sig ₅ (T, J)	5 · 22	0.496	109.3	112.1	115.7
Sig ₃ (T, J)	3 · 22	0.537	110.3	113.1	115.9
Sig ₅ (T)	5	0.505	109.7	112.4	115.9

Table 3: Comparison of different priors for aleatoric uncertainty in terms of MPJPE (mm) at 1 s on Human3.6M [28]. The stability refers to the variance of the training and the lower the better.

that taking aleatoric uncertainty into account with pUAL is beneficial and that a good choice of uncertainty prior is important. In particular, Sig₅ performs better than using no prior for all models. Using a prior can lead to similar aleatoric uncertainty than the unconstrained case, but with fewer learnable parameters and better stability.

5.5. Epistemic uncertainty

Evaluating the quality of epistemic uncertainty is difficult due to the unavailability of ground truth annotations. Selective classification is a widely used method to evaluate uncertainty quality, where a classifier has the option to refrain from classifying data points if its confidence level drops below a certain threshold [17]. We assess the performance of our epistemic uncertainty estimation using this method, and measure how well actions "sitting" and "sitting down" can be separated from actions "walking" and "walking together", all from the test set of Human3.6M, based solely on the predicted uncertainty of the model. The forecasting model and clustering are trained on Human3.6M walking-related actions, and we anticipate low uncertainty values for those actions and high uncertainty values for sitting-related actions, *i.e.*, not encountered and significantly distinct actions. During the assessment, we compute uncertainty scores for both actions and measure the classification results for a range of thresholds. Similar to prior research [51], we utilize the AUROC metric, where a higher score is desirable and a value of 1 indicates that all walking-related data points possess lower uncertainty than all sitting-related data points. In Tab. 4, we present our findings and compare them to alternative approaches, where our proposed method demonstrates higher AUROC. The full ROC curve is in Fig. 6. Note that our approach is model-agnostic in contrast to MC-Dropout. We present the results of further assessments of a broader range of actions in the appendix.

Another feature of our approach is computational efficiency, which is attributed to its ability to compute in a single forward path. This is in contrast to MC-Dropout and Ensemble methods. We provide a comparison of the average inference latency, measured in milliseconds, between our method and other approaches in Tab. 4. Our approach

Method	AUROC	Latency	Trainings
Deep-Ensemble-3	0.87	6.28	3
Deep-Ensemble-5	0.90	10.43	5
MC-Dropout-5	0.90	9.57	1
MC-Dropout-10	0.92	18.98	1
Ours	0.95	6.23	1

Table 4: AUROC, inference latency (ms) and number of training runs for different epistemic uncertainty methods.

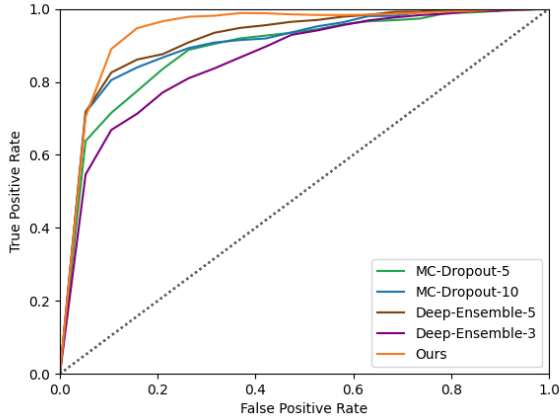


Figure 6: ROC curve for a model trained on walking-related actions and tested on both walking-related and sitting-related actions. The objective is to distinguish between these sets by utilizing uncertainty estimates.

shows lower latency and only requires one training. Notably, the performance gap between our approach and other methods may increase when using more computationally expensive forecasting models.

We conducted another experiment in Tab. 5 to showcase the effectiveness of our metric in out-of-distribution (OOD) motions. We shuffled the frames’ order (Frames shuffled) or joints (Joints shuffled) in each pose sequence of the test set to generate OOD data. The results demonstrate that our method identifies high uncertainties for Joints shuffled of all categories since they do not correspond to ID (in-distribution) poses. Furthermore, our approach yields high EpU values for almost all actions of Frames shuffled, compared to normal pose sequences, emphasizing the significance of frame order in generating an ID motion.

Additionally, we present the results of the models trained on AMASS in Table 6, in terms of A-MPJPE and EpU, on both the AMASS and 3DPW datasets. Note that the models and the clustering method were both trained on the AMASS dataset and therefore, higher uncertainties were recorded on 3DPW as an unseen dataset while prediction errors were lower. It indicates the reliability of forecasting models.

Action	Normal	Frames shuffled	Joints shuffled
Walking	0.26	1.35	2.15
Smoking	0.80	1.54	2.17
Posing	0.93	1.57	2.17
Directions	0.93	1.39	2.20
Greeting	0.81	1.50	2.17
Discussion	0.80	1.31	2.19
Walkingtogether	0.33	1.36	2.21
Eating	0.83	1.27	2.19
Phoning	0.82	1.56	2.20
Sitting	1.12	1.75	2.23
Waiting	0.82	1.57	2.15
Sittingdown	1.18	1.89	2.16
WalkingDog	0.95	1.53	2.20
TakingPhoto	1.02	1.47	2.17
Purchases	0.99	1.47	2.24
Average of all actions	0.85	1.53	2.18

Table 5: Comparison of EpU on different categories of Human3.6M. *Normal* refers to the original test set, *Frames shuffled* refers to the test set in which the frame orders in each sequence have been randomly shuffled, and *Joints shuffled* refers to randomly shuffled 3D joints in all frames.

Model	AMASS		3DPW	
	EpU	A-MPJPE	EpU	A-MPJPE
Zero-Vel	0.449	85.72	0.566	64.44
HRI [44]	0.351	43.76	0.463	43.62
STS-GCN [59]	0.332	45.49	0.455	42.60
ST-Trans + pUAL	0.336	35.86	0.439	40.02

Table 6: Comparison of different models in terms of A-MPJPE and EpU on AMASS [42] and 3DPW [65] datasets. The clustering and forecasting models were trained on AMASS [42].

6. Conclusion

In this paper, we focused on modeling the uncertainty of human pose forecasting. We suggested a method for modeling aleatoric uncertainty of pose forecasting models that could make state-of-the-art models uncertainty-aware and improve their performances. We showed the effect of uncertainty priors to inject knowledge about the behavior of uncertainty. Moreover, we measured the epistemic uncertainty of pose forecasting models by clustering poses into motion clusters, which enables us to evaluate the trustworthiness of victim models. We made an open-source library of human pose forecasting with several models, datasets, and metrics to move toward a unified and fair evaluation. As future work, we hope that the findings and the library will pave the way to more uncertainty-aware pose forecast-

ing models.

7. Acknowledgment

The authors extend their sincere gratitude to Armin Saadat and Nima Fathi for their invaluable contributions in the initial phase of the project and development of the library. Special thanks also go to Mohamad Asadi, Ali Rasekh, Megh Shukla and Mohammadhossein Bahari for their helpful input. This project has received funding from the European Union’s Horizon 2020 research and innovation programme under the Marie Skłodowska-Curie grant agreement No 754354, and SNSF Sinergia Fund.

References

- [1] Vida Adeli, Ehsan Adeli, Ian Reid, Juan Carlos Niebles, and Hamid Rezaatofghi. Socially and contextually aware human motion and pose forecasting. *IEEE Robotics and Automation Letters*, 5(4):6033–6040, 2020. 2
- [2] Sadegh Aliakbarian, Fatemeh Saleh, Lars Petersson, Stephen Gould, and Mathieu Salzmann. Contextually plausible and diverse 3d human motion prediction. In *IEEE/CVF International Conference on Computer Vision (ICCV)*, pages 11333–11342, October 2021. 2
- [3] Sadegh Aliakbarian, Fatemeh Sadat Saleh, Mathieu Salzmann, Lars Petersson, and Stephen Gould. A stochastic conditioning scheme for diverse human motion prediction. In *IEEE/CVF Conference on Computer Vision and Pattern Recognition (CVPR)*, pages 5223–5232, 2020. 2
- [4] Mohammadhossein Bahari, Saeed Saadatnejad, Ahmad Rahimi, Mohammad Shaverdikondori, Seyed-Mohsen Moosavi-Dezfooli, and Alexandre Alahi. Vehicle trajectory prediction works, but not everywhere. In *IEEE/CVF Conference on Computer Vision and Pattern Recognition (CVPR)*, 2022. 2
- [5] Lorenzo Bertoni, Sven Kreiss, and Alexandre Alahi. MonoLoco: Monocular 3D pedestrian localization and uncertainty estimation. In *IEEE/CVF International Conference on Computer Vision (ICCV)*, October 2019. 1, 3
- [6] Charles Blundell, Julien Cornebise, Koray Kavukcuoglu, and Daan Wierstra. Weight uncertainty in neural network. In *International conference on machine learning*, pages 1613–1622. PMLR, 2015. 3
- [7] Smail Bouhsain, Saeed Saadatnejad, and Alexandre Alahi. Pedestrian intention prediction: A multi-task perspective. In *European Association for Research in Transportation (hEART)*, 2020. 2
- [8] Yujun Cai, Yiwei Wang, Yiheng Zhu, Tat-Jen Cham, Jianfei Cai, Junsong Yuan, Jun Liu, Chuanxia Zheng, Sijie Yan, Henghui Ding, Xiaohui Shen, Ding Liu, and Nadia Magnenat Thalmann. A unified 3d human motion synthesis model via conditional variational auto-encoder. In *IEEE/CVF International Conference on Computer Vision (ICCV)*, pages 11645–11655, October 2021. 2
- [9] Zhe Cao, Hang Gao, Karttikeya Mangalam, Qi-Zhi Cai, Minh Vo, and Jitendra Malik. Long-term human motion prediction with scene context. In *European Conference on Computer Vision (ECCV)*, pages 387–404. Springer, 2020. 2
- [10] Yu-Wei Chao, Jimei Yang, Brian Price, Scott Cohen, and Jia Deng. Forecasting human dynamics from static images. In *IEEE/CVF Conference on Computer Vision and Pattern Recognition (CVPR)*, pages 548–556, 2017. 2
- [11] Changan Chen, Yuejiang Liu, Sven Kreiss, and Alexandre Alahi. Crowd-robot interaction: Crowd-aware robot navigation with attention-based deep reinforcement learning. In *International Conference on Robotics and Automation (ICRA)*, 2019. 1
- [12] Hsu-kuang Chiu, Ehsan Adeli, Borui Wang, De-An Huang, and Juan Carlos Niebles. Action-agnostic human pose forecasting. In *IEEE Winter Conference on Applications of Computer Vision (WACV)*, pages 1423–1432. IEEE, 2019. 2
- [13] Enric Corona, Albert Pumarola, Guillem Alenya, and Francesc Moreno-Noguer. Context-aware human motion prediction. In *IEEE/CVF Conference on Computer Vision and Pattern Recognition (CVPR)*, pages 6992–7001, 2020. 2
- [14] Qiongjie Cui, Huaijiang Sun, and Fei Yang. Learning dynamic relationships for 3d human motion prediction. In *IEEE/CVF Conference on Computer Vision and Pattern Recognition (CVPR)*, pages 6519–6527, 2020. 2
- [15] Lingwei Dang, Yongwei Nie, Chengjiang Long, Qing Zhang, and Guiqing Li. Msr-gcn: Multi-scale residual graph convolution networks for human motion prediction. In *IEEE/CVF International Conference on Computer Vision (ICCV)*, pages 11467–11476, 2021. 2, 5, 6
- [16] Nemanja Djuric, Vladan Radosavljevic, Henggang Cui, Thi Nguyen, Fang-Chieh Chou, Tsung-Han Lin, Nitin Singh, and Jeff Schneider. Uncertainty-aware short-term motion prediction of traffic actors for autonomous driving. In *IEEE Winter Conference on Applications of Computer Vision (WACV)*, pages 2084–2093, 2020. 2
- [17] Ran El-Yaniv et al. On the foundations of noise-free selective classification. *Journal of Machine Learning Research*, 11(5), 2010. 7
- [18] Katerina Fragkiadaki, Sergey Levine, Panna Felsen, and Jitendra Malik. Recurrent network models for human dynamics. In *IEEE/CVF International Conference on Computer Vision (ICCV)*, pages 4346–4354, 2015. 2
- [19] Yarin Gal and Zoubin Ghahramani. Dropout as a bayesian approximation: Representing model uncertainty in deep learning. In *International Conference on Machine Learning (ICML)*, pages 1050–1059. PMLR, 2016. 2, 3
- [20] Partha Ghosh, Jie Song, Emre Aksan, and Otmar Hilliges. Learning human motion models for long-term predictions. In *International Conference on 3D Vision (3DV)*, pages 458–466. IEEE, 2017. 2
- [21] Alex Graves. Practical variational inference for neural networks. *Advances in neural information processing systems*, 24, 2011. 3
- [22] Nitesh B. Gundavarapu, Divyansh Srivastava, Rahul Mitra, Abhishek Sharma, and Arjun Jain. Structured aleatoric uncertainty in human pose estimation. In *IEEE/CVF Conference on Computer Vision and Pattern Recognition (CVPR) Workshops*, June 2019. 2

- [23] Chuan Guo, Geoff Pleiss, Yu Sun, and Kilian Q Weinberger. On calibration of modern neural networks. In *International conference on machine learning*, pages 1321–1330. PMLR, 2017. 3
- [24] Chuchu Han, Xin Yu, Changxin Gao, Nong Sang, and Yi Yang. Single image based 3d human pose estimation via uncertainty learning. *Pattern Recognition*, 132:108934, 2022. 2
- [25] Mohamed Hassan, Duygu Ceylan, Ruben Villegas, Jun Saito, Jimei Yang, Yi Zhou, and Michael J. Black. Stochastic scene-aware motion prediction. In *IEEE/CVF International Conference on Computer Vision (ICCV)*, pages 11374–11384, October 2021. 2
- [26] Jian Hou and Marcello Pelillo. A new density kernel in density peak based clustering. In *2016 23rd International Conference on Pattern Recognition (ICPR)*, pages 468–473. IEEE, 2016. 4
- [27] Xin Huang, Stephen G. McGill, Brian C. Williams, Luke Fletcher, and Guy Rosman. Uncertainty-aware driver trajectory prediction at urban intersections. In *International Conference on Robotics and Automation (ICRA)*, pages 9718–9724, 2019. 2
- [28] Catalin Ionescu, Dragos Papava, Vlad Olaru, and Cristian Sminchisescu. Human3.6m: Large scale datasets and predictive methods for 3d human sensing in natural environments. *IEEE Transactions on Pattern Analysis and Machine Intelligence*, 36(7):1325–1339, jul 2014. 2, 5, 6, 7
- [29] Boris Ivanovic, Yifeng Lin, Shubham Shrivastava, Punarjay Chakravarty, and Marco Pavone. Propagating state uncertainty through trajectory forecasting. In *International Conference on Robotics and Automation (ICRA)*, pages 2351–2358, 2022. 2
- [30] Thorbjorn Mosekjær Iversen, Anders Glent Buch, and Dirk Kraft. Prediction of icp pose uncertainties using monte carlo simulation with synthetic depth images. In *IEEE/RSJ International Conference on Intelligent Robots and Systems (IROS)*, pages 4640–4647, 2017. 2
- [31] Ashesh Jain, Amir R Zamir, Silvio Savarese, and Ashutosh Saxena. Structural-rnn: Deep learning on spatio-temporal graphs. In *IEEE/CVF Conference on Computer Vision and Pattern Recognition (CVPR)*, pages 5308–5317, 2016. 2
- [32] Alex Kendall, Vijay Badrinarayanan, and Roberto Cipolla. Bayesian segnet: Model uncertainty in deep convolutional encoder-decoder architectures for scene understanding. *arXiv preprint arXiv:1511.02680*, 2015. 2
- [33] Alex Kendall and Yarin Gal. What uncertainties do we need in bayesian deep learning for computer vision? *Advances in Neural Information Processing Systems*, 30, 2017. 1, 2
- [34] Parth Kothari, Sven Kreiss, and Alexandre Alahi. Human trajectory forecasting in crowds: A deep learning perspective. *IEEE Transactions on Intelligent Transportation Systems*, 2021. 2
- [35] J. Kundu, S. Seth, P. YM, V. Jampani, A. Chakraborty, and R. Babu. Uncertainty-aware adaptation for self-supervised 3d human pose estimation. In *IEEE/CVF Conference on Computer Vision and Pattern Recognition (CVPR)*, pages 20416–20427, Los Alamitos, CA, USA, jun 2022. IEEE Computer Society. 2
- [36] Balaji Lakshminarayanan, Alexander Pritzel, and Charles Blundell. Simple and scalable predictive uncertainty estimation using deep ensembles. *Advances in neural information processing systems*, 30, 2017. 3
- [37] Chen Li, Zhen Zhang, Wee Sun Lee, and Gim Hee Lee. Convolutional sequence to sequence model for human dynamics. In *IEEE/CVF Conference on Computer Vision and Pattern Recognition (CVPR)*, pages 5226–5234, 2018. 1, 2, 5, 6, 7
- [38] Jeremiah Liu, Zi Lin, Shreyas Padhy, Dustin Tran, Tania Bedrax Weiss, and Balaji Lakshminarayanan. Simple and principled uncertainty estimation with deterministic deep learning via distance awareness. *Advances in Neural Information Processing Systems*, 33:7498–7512, 2020. 1, 3
- [39] Zhenguang Liu, Pengxiang Su, Shuang Wu, Xuanjing Shen, Haipeng Chen, Yanbin Hao, and Meng Wang. Motion prediction using trajectory cues. In *IEEE/CVF International Conference on Computer Vision (ICCV)*, pages 13299–13308, October 2021. 2
- [40] Hengbo Ma, Jiachen Li, Ramtin Hosseini, Masayoshi Tomizuka, and Chiho Choi. Multi-objective diverse human motion prediction with knowledge distillation. In *IEEE/CVF Conference on Computer Vision and Pattern Recognition (CVPR)*, pages 8161–8171, June 2022. 2
- [41] Tiezheng Ma, Yongwei Nie, Chengjiang Long, Qing Zhang, and Guiqing Li. Progressively generating better initial guesses towards next stages for high-quality human motion prediction. In *IEEE/CVF Conference on Computer Vision and Pattern Recognition (CVPR)*, pages 6437–6446, June 2022. 1, 2, 5, 6
- [42] Naureen Mahmood, Nima Ghorbani, Nikolaus F. Troje, Gerard Pons-Moll, and Michael J. Black. Amass: Archive of motion capture as surface shapes. In *IEEE/CVF International Conference on Computer Vision (ICCV)*, October 2019. 2, 5, 7, 8
- [43] Karttikeya Mangalam, Ehsan Adeli, Kuan-Hui Lee, Adrien Gaidon, and Juan Carlos Niebles. Disentangling human dynamics for pedestrian locomotion forecasting with noisy supervision. In *IEEE/CVF Winter Conference on Applications of Computer Vision*, pages 2784–2793, 2020. 1
- [44] Wei Mao, Miaomiao Liu, and Mathieu Salzmann. History repeats itself: Human motion prediction via motion attention. In *European Conference on Computer Vision (ECCV)*, pages 474–489. Springer, 2020. 1, 2, 5, 6, 7, 8
- [45] Wei Mao, Miaomiao Liu, and Mathieu Salzmann. Generating smooth pose sequences for diverse human motion prediction. In *IEEE/CVF International Conference on Computer Vision (ICCV)*, pages 13309–13318, 2021. 2
- [46] Wei Mao, Miaomiao Liu, Mathieu Salzmann, and Hongdong Li. Learning trajectory dependencies for human motion prediction. In *IEEE/CVF International Conference on Computer Vision (ICCV)*, October 2019. 1, 2, 5, 6, 7
- [47] Julieta Martinez, Michael J Black, and Javier Romero. On human motion prediction using recurrent neural networks. In *IEEE/CVF Conference on Computer Vision and Pattern Recognition (CVPR)*, pages 2891–2900, 2017. 2, 5, 6
- [48] RT McAllister, Yarin Gal, Alex Kendall, Mark Van Der Wilk, Amar Shah, Roberto Cipolla, and Adrian Weller.

- Concrete problems for autonomous vehicle safety: Advantages of bayesian deep learning. *International Joint Conferences on Artificial Intelligence, Inc.*, 2017. 2
- [49] Radford M Neal. *Bayesian learning for neural networks*, volume 118. Springer Science & Business Media, 2012. 2
- [50] Sergey Prokudin, Peter Gehler, and Sebastian Nowozin. Deep directional statistics: Pose estimation with uncertainty quantification. In *European Conference on Computer Vision (ECCV)*, Sept. 2018. 2
- [51] Jie Ren, Peter J Liu, Emily Fertig, Jasper Snoek, Ryan Poplin, Mark Depristo, Joshua Dillon, and Balaji Lakshminarayanan. Likelihood ratios for out-of-distribution detection. *Advances in neural information processing systems*, 32, 2019. 7
- [52] Charles Richter and Nicholas Roy. Safe visual navigation via deep learning and novelty detection. In *Robotics: Science and Systems*, 2017. 2
- [53] James H Ricketts and Geoffrey A Head. A five-parameter logistic equation for investigating asymmetry of curvature in baroreflex studies. *American Journal of Physiology-Regulatory, Integrative and Comparative Physiology*, 277(2):R441–R454, 1999. 4
- [54] H. Rong, A.P. Teixeira, and C. Guedes Soares. Ship trajectory uncertainty prediction based on a gaussian process model. *Ocean Engineering*, 182:499–511, 2019. 2
- [55] Saeed Saadatnejad, Mohammadhossein Bahari, Pedram Khorsandi, Mohammad Saneian, Seyed-Mohsen Moosavi-Dezfooli, and Alexandre Alahi. Are socially-aware trajectory prediction models really socially-aware? *Transportation Research Part C: Emerging Technologies*, 2022. 2
- [56] Saeed Saadatnejad, Yi Zhou Ju, and Alexandre Alahi. Pedestrian 3d bounding box prediction. In *hEART*, 2022. 2
- [57] Saeed Saadatnejad, Ali Rasekh, Mohammadreza Mofayezi, Yasamin Medghalchi, Sara Rajabzadeh, Taylor Mordan, and Alexandre Alahi. A generic diffusion-based approach for 3d human pose prediction in the wild. In *International Conference on Robotics and Automation (ICRA)*, 2023. 2
- [58] Tim Salzmann, Marco Pavone, and Markus Ryll. Motron: Multimodal probabilistic human motion forecasting. In *IEEE/CVF Conference on Computer Vision and Pattern Recognition (CVPR)*, pages 6457–6466, June 2022. 2
- [59] Theodoros Sofianos, Alessio Sampieri, Luca Franco, and Fabio Galasso. Space-time-separable graph convolutional network for pose forecasting. In *IEEE/CVF International Conference on Computer Vision (ICCV)*, pages 11209–11218, October 2021. 1, 2, 5, 6, 7, 8
- [60] Nitish Srivastava, Geoffrey Hinton, Alex Krizhevsky, Ilya Sutskever, and Ruslan Salakhutdinov. Dropout: a simple way to prevent neural networks from overfitting. *The journal of machine learning research*, 15(1):1929–1958, 2014. 3
- [61] Xiaolin Tang, Kai Yang, Hong Wang, Jiahang Wu, Yechen Qin, Wenhao Yu, and Dongpu Cao. Prediction-uncertainty-aware decision-making for autonomous vehicles. *IEEE Transactions on Intelligent Vehicles*, pages 1–15, 2022. 2
- [62] Yusuke Tashiro, Jiaming Song, Yang Song, and Stefano Ermon. Csd: Conditional score-based diffusion models for probabilistic time series imputation. *Advances in Neural Information Processing Systems*, 34:24804–24816, 2021. 5
- [63] Joost Van Amersfoort, Lewis Smith, Yee Whye Teh, and Yarin Gal. Uncertainty estimation using a single deep deterministic neural network. In *International conference on machine learning*, pages 9690–9700. PMLR, 2020. 1, 2, 3
- [64] Laurens van der Maaten and Geoffrey Hinton. Visualizing data using t-sne. *Journal of Machine Learning Research*, 9(86):2579–2605, 2008. 4
- [65] Timo von Marcard, Roberto Henschel, Michael J Black, Bodo Rosenhahn, and Gerard Pons-Moll. Recovering accurate 3d human pose in the wild using imus and a moving camera. In *European Conference on Computer Vision (ECCV)*, pages 601–617, 2018. 2, 5, 7, 8
- [66] Fabien B. Wagner, Jean-Baptiste Mignardot, Camille G. Le Goff-Mignardot, Robin Demesmaeker, Salif Komi, Marco Capogrosso, Andreas Rowald, Ismael Seáñez, Miroslav Caban, Elvira Pirondini, Molywan Vat, Laura A. McCracken, Roman Heimgartner, Isabelle Fodor, Anne Watrin, Perrine Seguin, Edoardo Paoles, Katrien Van Den Keybus, Grégoire Eberle, Brigitte Schurch, Etienne Pralong, Fabio Becce, John Prior, Nicholas Buse, Rik Buschman, Esra Neufeld, Niels Kuster, Stefano Carda, Joachim von Zitzewitz, Vincent Delattre, Tim Denison, Hendrik Lambert, Karen Minassian, Jocelyne Bloch, and Grégoire Courtine. Targeted neurotechnology restores walking in humans with spinal cord injury. *Nature*, 563(7729):65–71, Nov. 2018. 1
- [67] Jacob Walker, Carl Doersch, Abhinav Gupta, and Martial Hebert. An uncertain future: Forecasting from static images using variational autoencoders. In *European Conference on Computer Vision (ECCV)*, pages 835–851. Springer, 2016. 2
- [68] Jiali Wang, Yue Zhang, and Xv Lan. Automatic cluster number selection by finding density peaks. In *IEEE International Conference on Computer and Communications (ICCC)*, pages 13–18. IEEE, 2016. 4
- [69] Yiqi Wang, Zhan Shi, Xifeng Guo, Xinwang Liu, En Zhu, and Jianping Yin. Deep embedding for determining the number of clusters. In *AAAI Conference on Artificial Intelligence*, volume 32, 2018. 4
- [70] Yijun Xiao and William Yang Wang. Quantifying uncertainties in natural language processing tasks. In *Proceedings of the AAAI conference on artificial intelligence*, volume 33, pages 7322–7329, 2019. 2
- [71] Junyuan Xie, Ross Girshick, and Ali Farhadi. Unsupervised deep embedding for clustering analysis. In *International conference on machine learning*, pages 478–487. PMLR, 2016. 4
- [72] Sirui Xu, Yu-Xiong Wang, and Liang-Yan Gui. Diverse human motion prediction guided by multi-level spatial-temporal anchors. In *European Conference on Computer Vision (ECCV)*, 2022. 5, 6
- [73] Ye Yuan and Kris Kitani. Dlow: Diversifying latent flows for diverse human motion prediction. In *European Conference on Computer Vision (ECCV)*, 2020. 2
- [74] Jinlu Zhang, Yujin Chen, and Zhigang Tu. Uncertainty-aware 3d human pose estimation from monocular video. In *ACM International Conference on Multimedia*, pages 5102–5113, 2022. 2
- [75] Chongyang Zhong, Lei Hu, Zihao Zhang, Yongjing Ye, and Shihong Xia. Spatio-temporal gating-adjacency gcn for hu-

man motion prediction. In *IEEE/CVF Conference on Computer Vision and Pattern Recognition (CVPR)*, pages 6447–6456, June 2022. [2](#)